大韓土木學會論文集
第14卷 第1號 · 1994年 1月
pp. 195~202

가는 모래의 전단강도
-파괴포락선의 곡률특성과 상태정수에 관하여-

Shear Strength of Fine Sand
-Curvature Characteristics of Failure Envelope and Stress Parameter-

윤 여 원*
Yoon, Yeo Won

Abstract

In this research, a lot of triaxial test results (CID) are analyzed to study the curvature characteristics of failure envelope of sand and parametric relationship between shear strength and state parameter by Been and Jefferies. In the conventional triaxial tests, correction for the change of sectional area of a sample and for membrane influence is essential especially in order to determine critical state (or steady state) condition more correctly. Based on the test results, a model to express the shear strength of fine sand as a function of density and stress level is presented and curvature characteristics of shear failure envelope and parametric relationship between state parameter and shear strength parameters are evaluated.

요 지

본 연구에서는 모래의 전단파괴 포락선의 곡률특성을 구명하고 전단강도와 Been과 Jefferies가 제시한 상태정수간의 매개변수관계를 밝히기 위하여 많은 압밀배수삼축시험의 결과를 분석하였다. 통상적인 삼축시험에서 시료의 단면적 변화와 멤브레인의 영향에 대한 수정은 특히 한계상태를 결정하는데 중요하다고 할 수 있다. 실험결과로부터 전단강도를 밀도와 응력수준의 함수로 표현하는 모델을 제시하였고 모래의 전단파괴포락선의 곡률특성과 상태정수와 전단강도정수간의 관계를 밝혔다.

1. Introduction

The shear strength characteristics of sand vary not only with the density but also with the mean normal stress.[1,2] Therefore the secant angle of shear resistance, rather than tangent, should be accentuated.

Furthermore, properties of sand cannot be expressed in terms of relative density alone; a description of stress must also be included. Recently Been and Jefferies[3] proposed a state parameter, which offers some potential for the interpretation of many types of drained test results of cohesionless soils. It represents an adaptation of the parameter V_λ formerly proposed by Schofield and Wroth.[4] In this research the following items are

* 정회원 · 인하대학교 공과대학 토목공학과 전임강사

studied.

－shear strength as a function of mean normal stress and density (void ratio).

－evaluation of curvature characteristics of Mol sand.

－shear strength as a function of state parameter ψ.

2. Literature Review

2.1 Failure Criteria - Baligh's Criterion

After Yareshenko (1964) proposed an analytical expression for the failure envelope in Mohr diagram with power form, Baligh (1976)[5] formulated the criterion in the form of logarithmic relationship because of difficulties with Yareshenko's expression to assess the accuracy in representing the actual failure envelope for sands and in inadequacy for practical application. Baligh's criterion is the following (Fig. 1):

$$\tau_{ff}=\sigma_{ff}'\cdot\left[\tan\phi_o'+\tan\alpha_c\left(\frac{1}{2.3}-\log_{10}\frac{\sigma_{ff}'}{\sigma_{ref}}\right)\right] \qquad (1)$$

where

τ_{ff} = shear stress on the failure surface at failure

σ'_{ff} = effective normal stress on the failure surface at failure

σ_{ref} = arbitrary reference stress

ϕ'_o = secant effective shear angle at $\sigma'_{ff}=2.72\,\sigma_{ref}$

α_c = angle which describes the curvature of the failure envelope

$=\tan^{-1}(\Delta\tan\phi_s'/\Delta\log\sigma_{ff}')$

Here the secant effective shear angle was obtained from $\sin\phi'=(\sigma_1'-\sigma_3')/(\sigma_1'+\sigma_3')$ which defines ϕ' as the inclination of the tangent to Mohr circle through the origin. The curvature angle α_c is determined from the $\tan\phi_s$ versus $\log\sigma_{ff}$ plot (inclination of the slope).

As described by Baligh and Baldi et al.[6] on the basis of a large number of triaxial compression tests performed on silica sands, α_c increases with increasing relative density. Baldi et. al (1986) expressed the following empirical relationship for quartz sand:

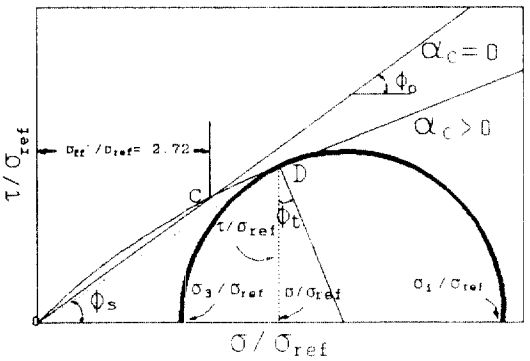

Fig. 1. Example of curved failure envelope.[5]

$$\alpha_c=[1.25\{D_r-A\}]\cdot 10^\circ \qquad (2)$$

where D_r = relative density

A = a constant depending on the compressibility characteristic of a sand, for silica sand $0.1\le A\le 0.2$.

2.2 Dilatancy

Sands at all initial densities will contract under constant uniform all-round pressure when sheared at low strain values; dense sands will dilate at larger strains and exhibit a brittle type stress-strain curve at low mean effective stress. When sheared at high confining pressures, the same dense sands will show much more contractive behavior and will exhibit a more plastic stress-strain relationship with high strains at failure.[7] It is therefore obviously not enough to use only relative density for describing sand behavior. It is indeed deficient in that it takes no account of the current state of stress. When a sand is strained beyond its peak shear strength, it reaches the critical state at large strains. At this stage further shear deformation occurs at constant volume or critical state value ϕ_{cv}' of the angle of friction.

The stress-dilatancy theory in essence states that in granular materials having a current void ratio e_o lower than that at critical state e_{cv} the difference between the mobilized secant shear angle ϕ_s' at peak and ϕ_{cv}' is controlled by the rate of dilation.

2.3 State Parameter ψ by Been and Jefferies

State parameter ψ (Fig. 2), which is defined as

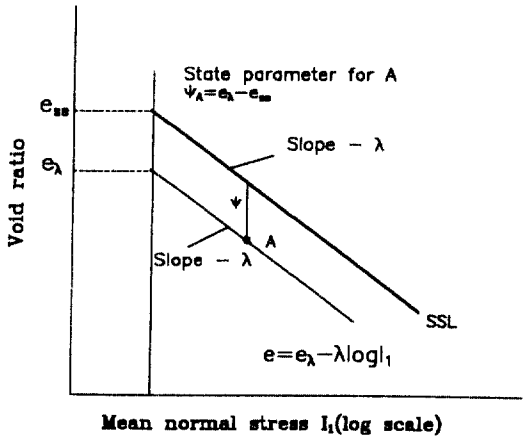

Fig. 2. Definition of state parameter by Been and Jefferies.[3]

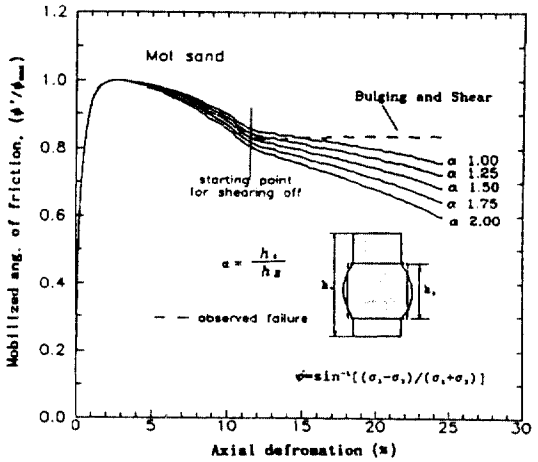

Fig. 3. Influence of area correction in terms of mobilized friction angle.

the void ratio difference between the initial p′−e state and steady state condition at the same mean effective stress p′, can be used to describe much of the behavior of granular materials over a wide range of stresses and densities. This parameter is embodied in the concept of critical state soil mechanics.

ψ represents an adaptation of the parameter V_λ (specific volume) formerly proposed by Schofield and Wroth (1968).

Samples with negative state parameter will always have a negative state at phase transformation and samples with high positive state parameter will have a positive state at phase transformation. For sands with negative parameter, there is a clean peak in deviatoric stress which becomes less marked with decreasing negative state parameter, until there is generally no peak for samples with positive state parameter. The volumetric strain behavior is similarly dependent on state parameter.

Strong dilation is apparent for high negative states with little dilation or even contraction observed where state parameter is positive.

3. Test Apparatus and Soil Type

The test equipment used in this research was a conventional triaxial apparatus with automatic data acquisition system. The sands involved in this research are obtained from a deposit at Mol, north-east of Belgium and composed of quartz minerals. Mol sand is a uniform, fine quartzitic sand with a median grain size of 0.195 mm, maximum void ratio of 0.918 and minimum void ratio of 0.585. All the triaxial tests (strain-controlled) were performed under CID condition on the sample of 10% water content and the ratio of sample height to diameter was 2.5. The specimen preparation of sand was done by undercompaction method (Ladd, 1972).

4. Experimental Results and Discussions

4.1 Influence of Sectional Area Change and Membrane

As already widely discussed and done by many scientists, secant angle of friction rather than tangent angle is used to express shear resistance throughout this research. Influence of membrane to the vertical and confining stress, and that of variation of sectional area to the vertical stress[8,9] were also considered.

Correction for the variation of sectional area, which can be classified mainly into cylindrical, parabolic, and barrel types, is very important in determining the point of steady state condition. The variations in strength with the choice of the failure type for the same sand are shown in Fig. 3. In that figure it is clear that at large deformation

the selection of failure type is very important. Therefore an appropriate choice of the area correction in this research was based on the observed geometry of the end of the tests. The corrected cross-sectional area is given by[8]

$$a_c = a_o\left[\frac{1-\varepsilon_v}{1-\alpha\varepsilon_a}\right] \quad \text{-cylindrical or barrel type}$$

$$a_c = a_o\left[-\frac{1}{4}+\frac{\sqrt{25-20\varepsilon_a-5\varepsilon_a^2}}{4(1-\varepsilon_a)}\right]^2 \quad \text{-parabolic type}$$

where

a_o = area corresponding to zero strain (after consolidation)

ε_v = volumetric strain

ε_a = axial strain

α = experimental constant, normally between 1 and 2 (see Fig. 3)

In the above equations, for both axial and volumetric strains, compressive strains are positive. For the cylindrical correction in the case of frictionless ends, the value of α is 1. Such bulging correction in the case of triaxial tests with frictional conventional porous stones, includes the value of α determined from the measurements after tests. σ is then defined as the ratio of the length of the specimen to the length of the bulging zone (Fig. 3). More detailed explanation can be obtained from the references.[2,8,9]

4.2 Dilatancy

As suggested from Rowe's stres-sdilatancy theory, the shear angle of friction can be related to dilatancy rate. From the test results, it can be seen in Fig. 4 that the maximum angle of friction is a function of dilatancy rate at failure (both volumetric strain and major principal strain are defined positive in compression). In the figure the shear angle at constant volume, ϕ_{cv}', is used as a material constant. The relationships between the shear angle and dilatancy rate for the sands tested are:

$$\phi' = 31.6 + 13.56(-d\varepsilon_v/d\varepsilon_1) \quad \text{with } \phi_{cv}' = 31.6 \qquad (3)$$

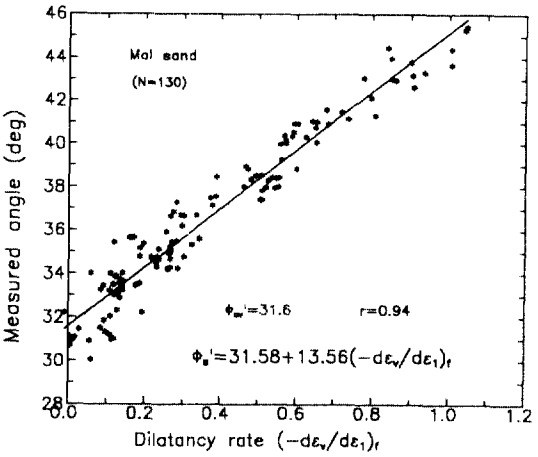

Fig. 4. The shear angle of friction in terms of dilatancy.

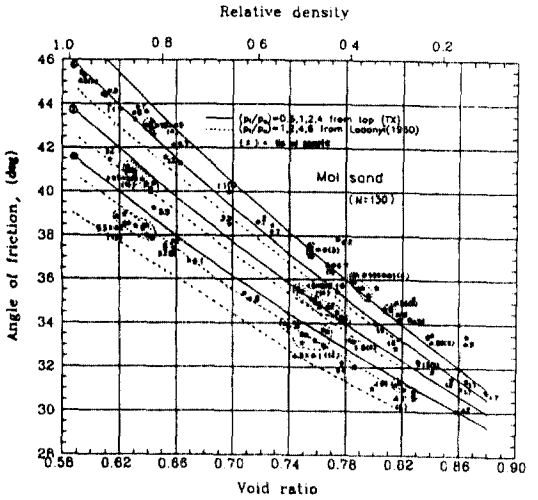

Fig. 5. The angle of friction as a function of mean normal stress and density.

in which ϕ' = the secant angle of friction.

4.3 Shear Strength as A Function of Density and Mean Normal Stress

The influence of normal stress level on the shear strength was recognized for a long time ago. In this research shear strength is expressed as a function of void ratio and and mean normal stress at failure, i.e. $\phi' = f(p_f', e)$. For the sands tested, the relationship (Fig. 5) may be stated as:

$$\phi' = A + B\cdot\ln\left(\frac{p_f'}{p_a}\right) \qquad (4)$$

where

p_f' = mean effective normal stress at failure

p_a = atmospheric pressure (1 kg/cm^2 = 98.1 kPa).

A, B = f(e)

In the above expression mean normal stress at failure was normalized by atmospheric pressure. Taking the data points from the approximated line (Fig. 5) with regular interval, the parameter A has best correlation with logarithm of void ratio while the parameter B has best correlated linearly with void ratio for the tested sands. Therefore

$$A = C_1 + C_2 \cdot \ln(e) \tag{5}$$

$$B = C_3 + C_4 \cdot (e) \tag{6}$$

The constants C_1, C_2, C_3 and C_4 in Eqs. (5) and (6) are shown in Table 1. The differences between the calculated values by the equation mentioned above and measured values are about 0.5°.

In the above expression the mean normal stress at failure can also be expressed as a function of confining stress at failure and shear angle of friction as follows (i.e., $\phi' = f(\sigma_c', e)$):

Consider the ratio of mean normal stress to deviatoric stress at failure for axisymmetric case

$$\frac{1}{3}\frac{(\sigma_1'+\sigma_2'+\sigma_3')}{(\sigma_1'-\sigma_3')} = \frac{1}{3}\left[\frac{(\sigma_1'+\sigma_3')}{(\sigma_1'-\sigma_3')} + \frac{\sigma_3'}{(\sigma_1'-\sigma_3')}\right] \tag{7}$$

According to Mohr-Coulomb criteria

$$(\sigma_1'-\sigma_3')/(\sigma_1'+\sigma_3') = \sin\phi' \tag{8}$$

Rearranging

$$\frac{\sigma_3'}{(\sigma_1'-\sigma_3')} = \frac{1}{2}\left(\frac{1}{\sin\phi'} - 1\right) \tag{9}$$

Substituting Eq.(9) into Eq.(7)

$$\frac{1}{3}\frac{(\sigma_1'+\sigma_2'+\sigma_3')}{(\sigma_1'-\sigma_3')} = \frac{1}{3}\left(\frac{3}{2}\frac{1}{\sin\phi'} - \frac{1}{2}\right) \tag{10}$$

From Eq. (9) $\sigma_1' = \sigma_3'(1+\sin\phi')/(1-\sin\phi')$. Substituting this into Eq. (10) and arranging

$$\frac{(\sigma_1'+\sigma_2'+\sigma_3')}{3} = \frac{\sigma_3'(3-\sin\phi')}{3(1-\sin\phi')} \tag{11}$$

Table 1. The constants C_1, C_2, C_3 and C_4 in Eqs. (5, 6)

C_1	C_2	C_3	C_4
25.70	−38.03	−7.48	7.46

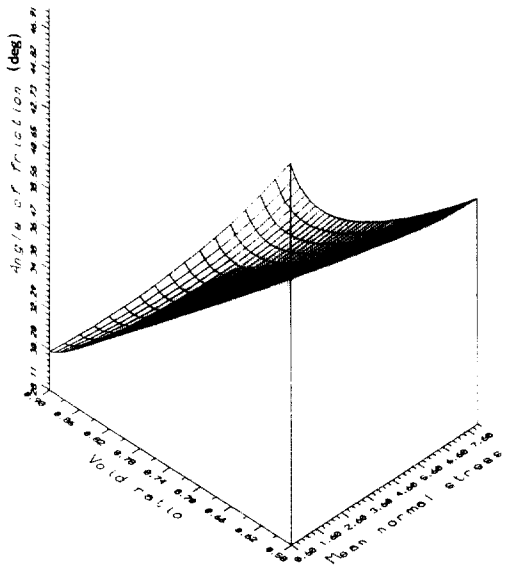

Fig. 6. 3-D view of $\phi' : e : p_f'$ relationship.

or

$$p_f' = \frac{\sigma_3'(3-\sin\phi')}{3(1-\sin\phi')}$$

Substituting this in Eq. (4), one gets finally

$$\phi' = f(e, \sigma_3') \tag{12}$$

4.4 Variation of Curvature Angle with Density of Sands

Taking some points from Eq. (4) and calculating the curvature angle by the definition in Section 3.1, the following vaules can be obtained.

Table 2. Curvature angle for various densities

e	0.62	0.66	0.70	0.74	0.78	0.82
α_c	11.8	9.9	8.3	6.8	5.6	4.4

From the table, it can be seen that curvature angle decreases with increasing void ratio (i.e., increases with increasing density). The variation of curvature angle with densities is plotted in Fig. 7 and the following relationship can be obtained.

$$\alpha_c = (3.42 - 3.67 \cdot e) \cdot 10^\circ \quad \text{or}$$

$$\alpha_c = (0.05 - 1.2 \cdot D_r) \cdot 10^\circ \qquad (13)$$

The results of Mol sands in this research are slightly higher than that of Baldi et al. The differences probably come from the determination method of maximum and minimum relative densities and from the different stress range of the data when the α_c is determined from the plot (i.e. in the regression analysis). The difference of 2 degrees in curvature angle is negligibly small.

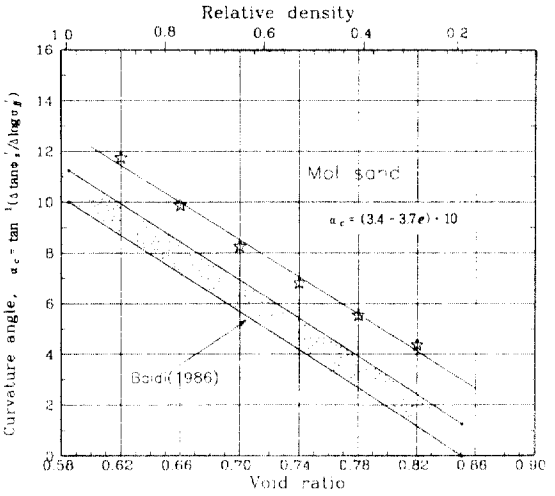

Fig. 7. Variation of curvature angle with densities.

4.5 Dependence of Shear Strength on the Present State of Stress

In this section, the behavior of sand is expressed in terms of the state parameters proposed by Schofield and Wroth (1968) and Been and Jefferies (1985) for the tested sand. The steady state of deformation for any mass of particles is that state in which the mass is continuously deforming at constant void ratio, constant normal effective stress, and constant velocity. In the present study the SSL were mainly obtained from CID tests and a few tests from CIU tests are added. In CIU tests the steady state condition was reached at large deformation with dilative behavior, while in CID tests such steady state was reached only when shear-plane failure happened at large deformation. The SSL for Mol sand is given in Fig. 8 and is expressed as the following.

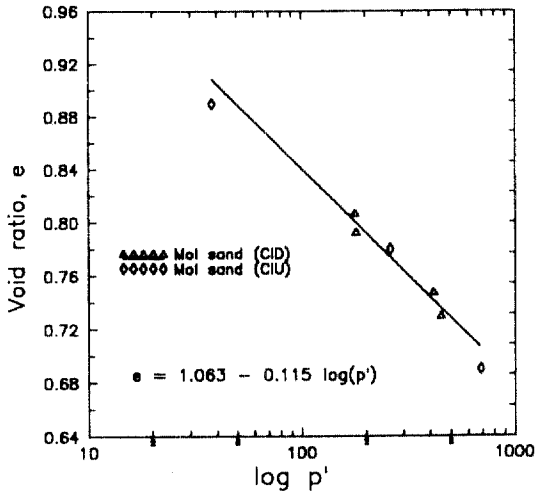

Fig. 8. The steady state line for Mol sand.

$$e = 1.063 - 0.115 \log p' \qquad (14)$$

in which p' = mean effective stress at steady state condition.

Based on the hypothesis that the SSL and CSL (critical state line) are defined by the same method (i.e., if there is no difference in physical condition except for terminological difference), the following relations between V_λ and ψ were established for the sand.

$$e_{ss} = 1.063;\ \lambda_{ss} = 0.115;\ V_\lambda - \psi = 1.833 \qquad (15)$$

where

e_{ss} = void ratio corresponding to $p' = 1$ kPa on the SSL.

λ_{ss} = slope of SSL (see Fig. 2)

V_λ = state parameter by Schofield and Wroth

4.6 The Shear Strength and Dilatancy as a Function of State Parameter

For the sands with negative ψ, the significant behavior is the drained angle of shear resistance

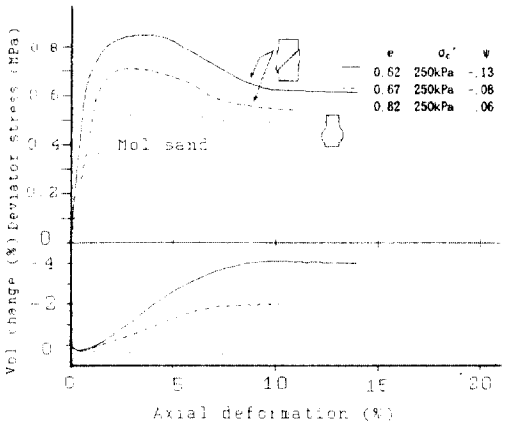

Fig. 9. Typical drained triaxial test result of Mol sand.[2]

and volumetric response. Typical drained triaxial test result on Mol sand is given in Fig. 9. For the sample of negative ψ, there are slightly clearer peak in the deviatoric stress; while it becomes less marked with decreasing parameter ψ. The volumetric strain behavior is similarly dependent on the state parameter. Strong dilatancy behavior is apparent for high negative value with little dilation observed where state parameter is positive.

Drained shear behavior of Mol sand as a function of state parameter is illustrated in Fig. 10. The angle of shear resistance is a well defined function of state parameter for the sands tested. The dilatancy rates for the sands tested as a function of state parameter are shown in Fig. 11. This relation is similar to shear angle versus state parameter plot.

5. Conclusions

From the interpretation of triaxial tests results on Mol sand, the following points might be concluded.

1) Shear angle of friction is a well-expressed function of dilatancy rate at failure as previous findings by other researchers.

2) The model to express the shear angle of friction of Mol sand as a function of density and mean normal stress at failure is presented as given by Eqs. (4, 5, 6) and Table 1.

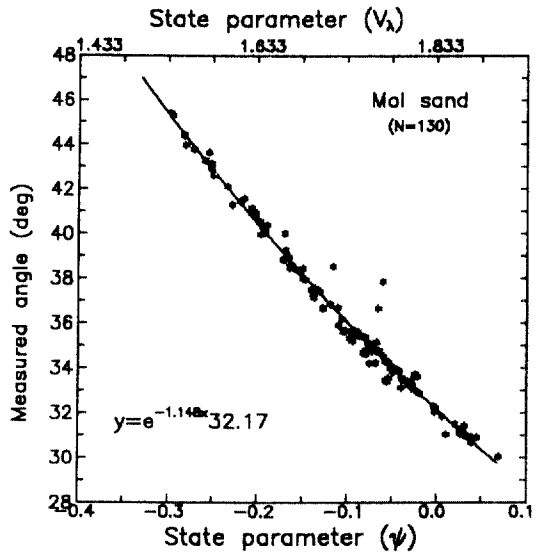

Fig. 10. The shear angle of friction as a function of state parameter.

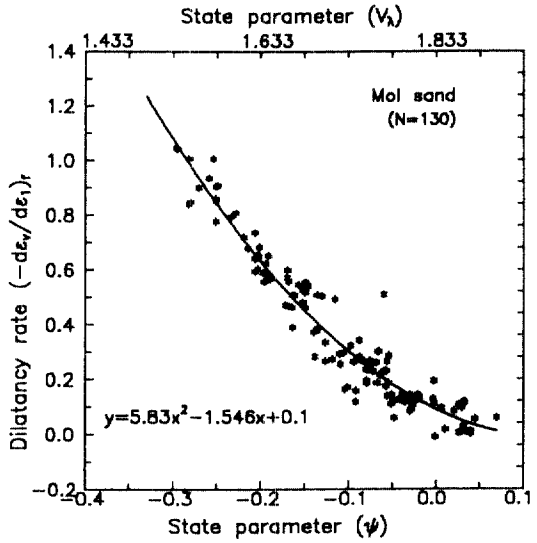

Fig. 11. Dilatancy rate at failure as a function of state parameter.

3) The curvature angle of Mol sand (α_c,) increases linearly with increasing density. as shown in Eq. (13).

3) State parameter, ψ, which combines void ratio and stress level, has a good correlation in connection with other parameters such as dilatancy

rate and peak friction angle for the tested results. The relationship confirmed the previous findings by Been and Jefferies (1985).

Acknowledgements

This research was completed by the support of research fund of Inha university. The data used in this research were obtained during the writer's stay in Ghent University (Belgium) as a part of exchange program. The writer thanks both universities.

References

1. Ladanyi, B., "Etude des relations entre les constraintes et les deformations lors du cissaillement des sols pulverulents," *Annales des Travaux Publics de Belgique*, Vol. No. 3, 1960.
2. Yoon, Y.-W., "Static and Dynamic Behavior of Crushable and Non-crushable Sands," Doctoral Thesis. Ghent University, Belgium, 1991.
3. Been, K. and Jefferies, M.G., "A State Parameter for Sands," *Geotechnique*, Vol. 35, No. 2, 1985, pp. 99~112.
4. Schofield, A.N. and Wroth, C.P., *Critical State Soil Mechanics*, McGraw-Hill Book Co., Inc., 1968.
5. Baligh, M.M., "Cavity Expansion in Sands with Curved Envelopes," *Journal of the Geotechnical Engineering Division*, ASCE, Vol. 102, No. GT11, Nov. 1976, pp. 1131~1146.
6. Baldi et al., "Interpretation of CPT's and CPTU's 2nd part: Drained Penetration of Sands," *4th Int'l Geotechnical Seminar on Field Instrumentation and In-Situ Measurements*, 1986, pp. 143~156.
7. Lee, K.L., "Drained Strength Characteristics of Sands," *Journal of the Soil Mechanics and Foundations Division*, ASCE, Vol. 93, No. SM6, Nov. 1967, pp. 117~141.
8. Germaine, J.T. and Ladd, C.C., "Triaxial Testing of Saturated Cohesive Soils," *Advanced Triaxial Testing of Soil and Rock*, ASTM STP 977, 1988, pp. 421~459.
9. La Rochelle et al., "Observational Approach to Membrane and Area Corrections in Triaxial Tests," *Advanced Triaxial Testing of Soil and Rock*, ASTM STP 977, 1988, pp. 715~731.

(接受 : 1993. 8. 11)